J|A|C|S
ARTICLES
Published on Web 04/28/2007

Adsorption Energy, Growth Mode, and Sticking Probability of Ca on Poly(methyl methacrylate) Surfaces with and without Electron Damage

Junfa Zhu, Paul Goetsch, Nancy Ruzycki, and Charles T. Campbell*

Contribution from the Department of Chemistry, University of Washington, Seattle, Washington 98195-1700

Received October 17, 2006; E-mail: campbell@chem.washington.edu

Abstract: The adsorption of Ca atoms on pristine and electron-irradiated poly(methyl methacrylate) (PMMA) surfaces at 300 K has been studied by adsorption microcalorimetry, atomic beam/surface scattering, and low-energy He^+ ion scattering spectroscopy (ISS). On pristine PMMA, the initial sticking probability of Ca is 0.5, increasing quickly with Ca coverage. Below 0.5 ML, the heat of adsorption is 730−780 kJ/mol, much higher than Ca's sublimation energy (178 kJ/mol). The Ca here is invisible to ISS, which is attributed to Ca binding to ester groups below the CH_3/CH_2-terminated PMMA surface. The adsorption energy increases with coverage, suggesting attractions between neighboring Ca−ester complexes. Above 0.5 ML, Ca starts to grow as three-dimensional (3D) Ca clusters on top of the surface, which dominate growth after 2 ML. It is proposed that each Ca reacts with two esters to form the Ca carboxylate of PMMA, because this reaction's heat would be close to that observed. The total amount of Ca that binds to subsurface sites is estimated from the integral heat of adsorption to involve 4−6 layers of ester groups. Exposing the PMMA surface to electrons increases Ca's initial sticking probability but lowers its adsorption energy. This is attributed to electron-induced defects acting as nucleation sites for 3D Ca islands, whose growth now competes kinetically with Ca diffusing to subsurface esters. Consequently, only two layers of subsurface esters get populated at saturation. The heat eventually reaches Ca's bulk heat of sublimation on all PMMA surfaces, where pure, bulk-like Ca thin films form.

1. Introduction

Metal/polymer interfaces play a crucial role in many important technological applications such as coatings, molecular electronic and optoelectronic devices, and semiconductor packaging.[1−3] These applications have stimulated years of substantial fundamental research on metal/polymer interfaces, using standard surface and interface analysis techniques including XPS, AFM, TEM, and HREELS, etc. Most of these studies have focused on the reaction, diffusion, and surface morphology of vapor deposited metal thin films on polymer surfaces.[4−7] Very little is known about the strength and the energetics of chemical bonding at the metal/polymer interface, which are key parameters for understanding metal/polymer interactions and for determining the strength of the interface.

PMMA is one of the most widely used polymers in manufacturing. It is used in photolithography,[8] biomedical implants,[9] barriers, membranes, and optical applications.[10] The ester group is generally accepted as the key chemically active unit in promoting metal interactions,[11−13] as seen in the structure of PMMA (shown in the insertion of Figure 1). Calcium deposition onto polymer surfaces is of considerable importance to a number of applications, especially in polymer light emitting devices (LEDs), where calcium is often used as an electrode in these devices because it has a relatively low work function (2.87 eV) and enhances the light emission.[14,15] So far, there have been extensive studies carried out on the interactions of Ca with the surfaces of various polymers including oxygen-containing polymers, for example, Ca on PPV,[16,17] and also a variety of studies of the interactions of other metals with PMMA, for example, Cu on PMMA.[18] However, to our knowledge, no prior studies of the Ca/PMMA interaction have been reported.

(1) Wong, C. P. *Polymers for Electronic and Photonic Applications*; Academic Press: Boston, 1993.
(2) Tabata, Y.; Mita, I.; Nonogaki, S.; Horie, K.; Tagawa, S. *Polymers for Microelectronics*; VCH Weinheim: New York, 1990.
(3) Bharathan, J. M.; Yang, Y. *J. Appl. Phys.* **1998**, *84*, 3207.
(4) Pireaux, J. J. *Synth. Met.* **1994**, *67*, 39.
(5) Faupel, F.; Willecke, R.; Thran, A. *Mater. Sci. Eng., R* **1998**, *22*, 1.
(6) Kurmaev, E. Z.; Moewes, A.; Ederer, D. L. *X-Ray Spectrom.* **2002**, *31*, 219.
(7) Zaporojtchenko, V.; Strunskus, T.; Behnke, K.; Von Bechtolsheim, C.; Kiene, M.; Faupel, F. *J. Adhes. Sci. Technol.* **2000**, *14*, 467.
(8) Kuan, S. W. J.; Frank, C. W.; Yen Lee, Y. H.; Eimori, T.; Allee, D. R.; Pease, R. F. W.; Browning, R. *J. Vac. Sci. Technol., B* **1989**, *7*, 1745.
(9) Park, J. B.; Lakes, R. S. *Biomaterials: an Introduction*; Plenum Press: New York, 1992.
(10) *Molecular Engineering of Ultrathin Films*; Stroeve, P., Franses, E. I., Eds.; Elsevier: London, 1987.
(11) Oultache, A. K.; Prud'homme, R. E. *Polym. Adv. Technol.* **2000**, *11*, 316.
(12) Bebin, P.; Prud'Homme, R. E. *J. Polym. Sci., Part B: Polym. Phys.* **2002**, *40*, 82.
(13) Bebin, P.; Prud'Homme, R. E. *Chem. Mater.* **2003**, *15*, 965.
(14) Braun, D.; Heeger, A. J. *Appl. Phys. Lett.* **1991**, *58*, 1982.
(15) Gustafsson, G.; Cao, Y.; Treacy, G. M.; Klavetter, F.; Colaneri, N.; Heeger, A. J. *Nature* **1992**, *357*, 477.
(16) Gao, Y.; Park, K. T.; Hsieh, B. R. *J. Chem. Phys.* **1992**, *97*, 6991.
(17) Andersson, G. G.; van Gennip, W. J. H.; Niemantsverdriet, J. W.; Brongersma, H. H. *Chem. Phys.* **2002**, *278*, 159.
(18) Bertrand, P.; Lambert, P.; Travaly, Y. *Nucl. Instrum. Methods Phys. Res., B* **1997**, *131*, 71.

10.1021/ja067437c CCC: $37.00

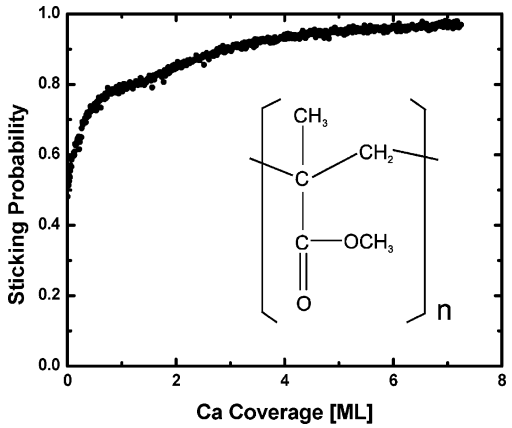

Figure 1. The measured sticking probability of Ca onto a pristine, spin-coated PMMA surface as a function of Ca coverage at 300 K. Each data point represents a pulse of approximately 0.006 ML of Ca coverage at a pulse frequency of $^1/_2$ Hz. This is the average of three reproducible experimental runs. The inset shows the structure of poly(methyl methacrylate) (PMMA).

Metal adsorption microcalorimetry directly measures the energy difference between the gaseous metal atoms and these atoms after they have bonded onto the probe surfaces, irrespective of the nature of the probe surfaces.[19] It has been successfully applied to study the energetics of metals adsorption onto various substrates including metal single crystal[20−24] and oxide[25−31] surfaces. Recently, we developed a new technique using microcalorimetry to measure the energy released as the metal−polymer bonds form upon metal adsorption, while simultaneously measuring the sticking probability.[32] Together, these provide direct information regarding the strength of metal/polymer chemical bonding, which is also immediately related to their adhesion energy. With this technique, we performed the first complete microcalorimetric studies of any metal on any polymer surface where the sticking probably was also measured, Pb adsorption on poly(methyl methacrylate) (PMMA) surfaces.[32]

Here, we present the first application of this technique to measure the adsorption energies of any reactive metal on any polymer surface by studying calcium adsorption on PMMA surfaces. In contrast to the Pb on PMMA case, where the metal does not react with the polymer but instead only forms 3D solid Pb particles on the surface,[32] Ca reacts very strongly with PMMA surface initially. Combining this with measurements of sticking probability and low-energy He^+ ion scattering spectroscopy, we are able to propose the first model of how Ca atoms bond to PMMA surfaces, and one of the more complete pictures of metal bonding to any polymer surface. The results reveal a surprising subsurface Ca species that was not expected.

This is the first study of Ca interactions with any polymer's surface wherein the adsorption energetics have been measured calorimetrically together with the metal atom's sticking probability. Measurements of the heat of adsorption of Ca on poly-[2-methoxy,5-(2′-ethylhexyloxy)-*p*-phenylene-vinylene] (MEH-PPV) and poly[2-methoxy,5-(2′-ethylhexyloxy)-*p*-phenylene] (MEH-PP) and pyromellitic dianhydride-oxidianiline (PMDA-ODA) polyimide have been reported previously, but in those cases it was assumed that the sticking probability of the Ca atoms on the polymers was unity.[33,34] We show here that the initial sticking probability of Ca on PMMA is only 0.5, which means that the initial heat of adsorption resulting from making that same assumption here would be in error by 50%, or 380 kJ/mol too low.

2. Experimental Section

The calorimetry methods for measuring the adsorption energies of metal particles on polymer surfaces have been described in detail previously.[32] Briefly, the calorimeter is housed in an ultrahigh vacuum analysis chamber with a base pressure of 2×10^{-10} mbar, which is equipped with a hemispherical electron energy analyzer (Leybold-Heraeus EA 11/100) for Auger electron spectroscopy (AES) and ion scattering spectroscopy (ISS), a UTI quadrupole mass spectrometer (QMS), an ion gun (LK Technologies), and a quartz crystal microbalance (QCM). This analysis chamber and the pulsed metal atomic beam are the same as those described elsewhere.[19] A small sample preparation chamber where multiple samples can be stored, outgassed, and transferred into the analysis chamber is adjacent to the analysis chamber.[32] It has a base pressure of 8×10^{-9} mbar.

The heat detector of the calorimeter is a highly sensitive Al-coated 9 μm-thick pyroelectric β-polyvinylidene fluoride (PVDF). It was cut into a 1.3 cm diameter circular sheet from a large sheet of metal-coated PVDF (Measurement Specialties, Inc.) with ceramic scissors to avoid face-to-face shorts. PMMA (MW = 15 000 amu, Sp^2 Scientific Polymer Products, Inc.) was directly spin-coated onto the PVDF sheet from a PMMA solution in chloroform (5.2% w/v) with 2000 rpm for 30 s. The estimated film thickness is 1.0 μm.[35] The morphology of these thin PMMA films, monitored by atomic force microscopy, was flat and homogeneous (root-mean-square roughness = 0.4 ± 0.1 nm on a 1×1 μm^2 area). Each freshly spin-coated PMMA sample was first mounted on the specially designed sample platen (see ref 32), placed on the platen carriage in the sample preparation chamber, and evacuated to below 3×10^{-8} Torr. Next, it was heated to 335 K for 24 h before measurements and to 350 K for 30 min just before use to remove the excess solvent and surface contaminants; these temperatures are below the glass transition temperature of PMMA (T_g = 391 K). Usually eight such samples were prepared at the same time. An AES spectrum of a representative sample did not show a Cl peak, indicating that this is sufficient to completely remove the spin coating solvent. Detailed information about polymer sample preparation, sample platen, and multiple sample carriage can be found in ref 32.

The calorimeter measures the peak-to-peak output voltage that is the response of the PVDF detector to a heat pulse arising from adsorbing pulses of Ca gas atoms onto the PMMA surface. This voltage is then converted into energy by calibrating the response to pulses of known

(19) Stuckless, J. T.; Frei, N. A.; Campbell, C. T. *Rev. Sci. Instrum.* **1998**, *69*, 2427.
(20) Stuckless, J. T.; Starr, D. E.; Bald, D. J.; Campbell, C. T. *J. Chem. Phys.* **1997**, *107*, 5547.
(21) Stuckless, J. T.; Starr, D. E.; Bald, D. J.; Campbell, C. T. *Phys. Rev. B* **1997**, *56*, 13496.
(22) Zhu, J. F.; Diaz, S. F.; Heeb, L. R.; Campbell, C. T. *Surf. Sci.* **2005**, *574*, 34.
(23) Starr, D. E.; Ranney, J. T.; Larsen, J. H.; Musgrove, J. E.; Campbell, C. T. *Phys. Rev. Lett.* **2001**, *87*, art. no. 106102
(24) Larsen, J. H.; Starr, D. E.; Campbell, C. T. *J. Chem. Thermodyn.* **2001**, *33*, 333.
(25) Campbell, C. T.; Starr, D. E. *J. Am. Chem. Soc.* **2002**, *124*, 9212.
(26) Campbell, C. T.; Parker, S. C.; Starr, D. E. *Science* **2002**, *298*, 811.
(27) Larsen, J. H.; Ranney, J. T.; Starr, D. E.; Musgrove, J. E.; Campbell, C. T. *Phys. Rev. B* **2001**, *63*, art. no. 195410.
(28) Ranney, J. T.; Starr, D. E.; Musgrove, J. E.; Bald, D. J.; Campbell, C. T. *Faraday Discuss.* **1999**, *114*, 195.
(29) Starr, D. E.; Campbell, C. T. *J. Phys. Chem. B* **2001**, *105*, 3776.
(30) Starr, D. E.; Bald, D. J.; Musgrove, J. E.; Ranney, J. T.; Campbell, C. T. *J. Chem. Phys.* **2001**, *114*, 3752.
(31) Starr, D. E.; Diaz, S. F.; Musgrove, J. E.; Ranney, J. T.; Bald, D. J.; Nelen, L.; Ihm, H.; Campbell, C. T. *Surf. Sci.* **2002**, *515*, 13.
(32) Diaz, S. F.; Zhu, J. F.; Harris, J. J. W.; Goetsch, P.; Merte, L. R.; Campbell, C. T. *Surf. Sci.* **2005**, *598*, 22.
(33) Hon, S. S.; Richter, J.; Stuckless, J. T. *Chem. Phys. Lett.* **2004**, *385*, 92.
(34) Murdey, R.; Stuckless, J. T. *J. Am. Chem. Soc.* **2003**, *125*, 3995.
(35) Walsh, C. B.; Frances, E. I. *Thin Solid Films* **1999**, *347*, 167.

energy from a He−Ne laser that passes through the same collimating path as the Ca metal beam. The reflectivity of each sample for the He−Ne laser was measured ex-situ using an integrating sphere and was found to be 0.87. The peak-to-peak voltage response of the detector has been proven to be linear over the energy range observed during the experiments. The sensitivity of the directly spin-coated PMMA on the detector is 450 V/J_{abs} (volts per joule of heat absorbed by the PMMA).

The metal atom beam is produced from 99.5% purity Ca granules (Alfa Aesar), which is evaporated from an effusive vapor source containing an alumina-lined tungsten crucible. The beam emitted from the metal source is collimated to provide a 4 mm diameter deposition area on the PMMA sample and is chopped into 100 ms long pulses at $^1/_2$ Hz. This results in a heat detector voltage pulse that rises to a maximum in 100 ms and decays to one-half its maximum 350 ms later. Each metal pulse contains 0.004−0.006 ML of Ca. One ML (monolayer) is defined here as 7.4×10^{14} atoms/cm^2, which is the packing density of solid Ca's closest-packed crystal surface, the <111> face. The operating temperature of the oven is 1000 K, which generates some thermal radiation that impinges on the sample and also is detected by the calorimeter (0.07 μJ/pulse, or 72.8 ± 0.4 kJ of absorbed radiation per mole of dosed Ca). This radiation was measured by blocking the metal beam with a BaF_2 window, which blocks the metal atoms from impinging onto the PMMA surface but passes a known fraction of the radiation (95%, measured before and after each experiment with laser pulses detected by the calorimeter). This radiation contribution is subtracted from the total measured signal. To convert these measured internal energy changes into standard enthalpy changes at the sample temperature (300 K), the excess translational energy of the metal gas atoms at the oven temperature, above that for a 300 K Maxwell−Boltzmann distribution (0.05 μJ/pulse), is subtracted, and a small pressure−volume work term (RT per mole) is added, as described elsewhere.[19] This corrected standard enthalpy of adsorption measured at high coverage, where the atoms are adding to bulk-like sites, is thus directly comparable to the standard heat of sublimation of the metal. The measured heats can be expressed as the energy of adsorption on a "per mole adsorbed metal" by dividing the amount of adsorbed Ca in each pulse, which is obtained by correcting the absolute Ca beam flux (measured using a calibrated quartz crystal microbalance) with the experimentally determined sticking probability. The sticking probability is measured by a modified King−Wells method, using a line-of-sight quadrupole mass spectrometer (QMS) at the so-called magic angle (35° from the surface normal) to measure the fraction of metal atoms that strike the surface but do not adsorb. A zero-sticking reference signal is provided by measuring the integrated desorption of a known amount of multilayer Ca on a Ta foil, located at the same position as the sample, corrected for average velocity.[19]

The sample reflectivity changes due to Ca adsorption. This must be measured to accurately calculate the changes in the amount of radiation absorbed by the sample as a function of coverage. There are two methods that can be used to measure the changes of the sample reflectivity as a function of coverage, as described in ref 30. One is to measure the change in detector response to optical heat from the He−Ne laser as a function of coverage, and the other is to measure the total angular-integrated change in reflectivity. Here, we used the first method to measure the Ca-coverage-dependent sample response (heat signal) to light pulses of fixed intensity, from which the relative changes in absorbency (reflectivity) as a function of Ca coverage can be extracted.

Ion scattering spectroscopy (ISS) was performed to monitor the growth mode of Ca atoms on the PMMA surface. All ISS experiments were carried out using $^4He^+$ ions with 1 keV primary energy. The helium gas was introduced through a non-focused ion sputter gun (LK Technologies) with a background He pressure of 7×10^{-7} Torr. The sample was positioned perpendicular to the electron/ion analyzer, and the ion beam was directed at 45° with respect to the surface normal. The analyzer detection mode was constant retarding ratio mode ($\Delta E/E = 4$). To minimize sample damage by ions, the sample was exposed to ions only during spectrum acquisition (~80 s). For measurements of Ca growth on PMMA, each deposition of Ca followed previous depositions in a consecutive way, starting with a pristine PMMA sample. To check the possible effect of cumulative He^+ ion damage on the growth model, new samples deposited in one step to several Ca coverages were measured using ISS; these intensities were compared to the values measured from the consecutively deposited sample at the same Ca coverage and were found to agree within the error bar (<5%).

PMMA is an insulating sample. To minimize the charging effect on the ISS spectra, a positive 5 V bias voltage was applied to its underlying metal electrode during ISS measurements.

3. Results

3.1. Ca on Pristine PMMA.

3.1.1. Sticking Probability. Figure 1 shows the sticking probability of Ca on the pristine PMMA surface at 300 K as a function of Ca coverage. (This coverage axis is the amount of Ca actually adsorbed on the surface after correcting for the sticking probability.) The data are an average of three experiments. Here, the "pristine" surface refers to the sample after regular degassing and transferring to the analysis chamber without exposing the sample to any electrons or ions. To avoid electron damage to the PMMA surface from the hot filament of the mass spectrometer during the experiments, a metal mesh with a negative 500 V bias voltage was placed between the sample and the mass spectrometer. No other electron sources were present. (The ion gauge was separated from the PMMA such that several wall collisions would be required for its electrons to reach the PMMA.) The sticking probability starts initially at 0.48 and increases rapidly with Ca coverage to 0.7 at 0.5 ML. Thereafter, it increases only very slowly with Ca coverage to 0.81 at 2 ML, but accelerates with further Ca deposition beyond 2 ML, then asymptotically approaches unity. By multiplying the measured sticking probability with the corresponding dosed amount of Ca in a pulse, the total amount of Ca adsorbed on the PMMA surface in each pulse was obtained. Those Ca atoms that do not stick on the PMMA surface either scatter quasi-elastically from the solid or are transiently adsorbed in a weakly held precursor but desorb again rapidly.

Comparison of the line shape of the quadrupole mass spectrometer response from desorbed metal beam pulses to the instrument response function (not shown) indicates that the residence time of any transiently adsorbed metal species on the surface (as observed by the decay in their signal at the end of a pulse) is less than 5 ms, the response time of the beam chopper cutoff, for the observed coverages.[36] This lifetime implies that, if they are transiently adsorbed, they have a heat of adsorption less than 79 kJ/mol, assuming a typical desorption rate constant prefactor of 10^{16} s^{-1}.[37]

3.1.2. ISS Experiments. Growth of metal films on polymer surfaces has been found to produce a variety of structures, including 3D metal particles, continuous metal films, and even subsurface metal.[13,38−41] Understanding the growth of Ca on

(36) Starr, D. E. Microcalorimetric heats of adsorption, surface residence times and stick probabilities of metals on metal-oxide, and silicon substrates. Ph.D. thesis, University of Washington, Seattle, 2001.
(37) Campbell, C. T.; Sun, Y. K.; Weinberg, W. H. *Chem. Phys. Lett.* **1991**, *179*, 53.
(38) Strunskus, T.; Zaporojtchenko, V.; Behnke, K.; von Bechtolsheim, C.; Faupel, F. *Adv. Eng. Mater.* **2000**, *2*, 489.
(39) Strunskus, T.; Kiene, M.; Willecke, R.; Thran, A.; Bechtolsheim, C. v.; Faupel, F. *Mater. Corros.* **1998**, *49*, 180.

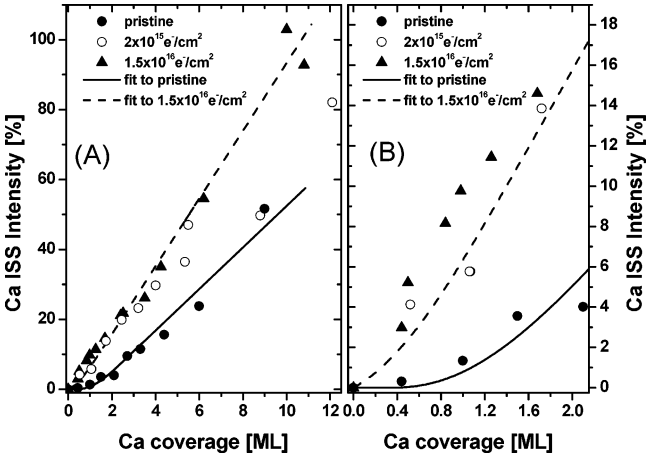

Figure 2. The evolution of the Ca peak intensity in low-energy He^+ ion scattering spectroscopy (ISS) as a function of Ca coverage for pristine and electron-irradiated PMMA surfaces at 300 K. The filled circles (●) are experimental data for pristine PMMA, the open circles (○) are experimental data for an electron dose of 2×10^{15} e^-/cm^2, and the filled triangles (▲) are experimental data for an electron dose of 1.5×10^{16} e^-/cm^2. The solid and dashed lines are the fits to these data using the two-site model described in the text, wherein the coverages of Ca deposited into each site were calculated from the measured heat of adsorption at each pulse. The solid line is for pristine PMMA, while the dashed line is for PMMA with an electron dose of 1.5×10^{16} e^-/cm^2. The right panel (B) shows an expanded view of the low-coverage region.

PMMA will help to interpret the measured coverage-dependent heats of adsorption. Low-energy He^+ ion scattering spectroscopy is a good technique for probing the growth of Ca on PMMA because it provides elemental analysis sensitive only to the topmost atomic layer.[42,43] Our pristine PMMA surface showed very low intensities for both C and O peaks in ISS. As has been proposed previously based on more detailed ISS studies of spin-coated PMMA,[18,44,45] its surface exposes mainly methyl and methylene groups, and its ester groups reside mainly below the surface. This minimizes the surface energy.[18,46] These methyl and methylene groups thus mask most of the ISS signal from O atoms, and their H atoms (which really terminate the surface) mask the ISS signal from the C atoms. (In ISS with He ions of this kinetic energy, signal "masking" really occurs due to efficient neutralization of the He^+ ions by the electrons of the masking atoms.)

Shown in Figure 2 is the evolution of the Ca ISS peak intensity for Ca adsorption on the pristine PMMA surface (●) as a function of the Ca coverage that actually adsorbed on the surface (after correcting for the sticking probability). As seen, below 1 ML, the intensity of the Ca peak increases very slowly, suggesting that most of the Ca atoms are hidden below the topmost atomic layer. This we attribute to Ca binding to the oxygen atoms of subsurface ester groups. After 1.5 ML, the Ca intensity starts to increase at a faster rate, indicating that Ca atoms begin to populate sites on the topmost surface layer. Even

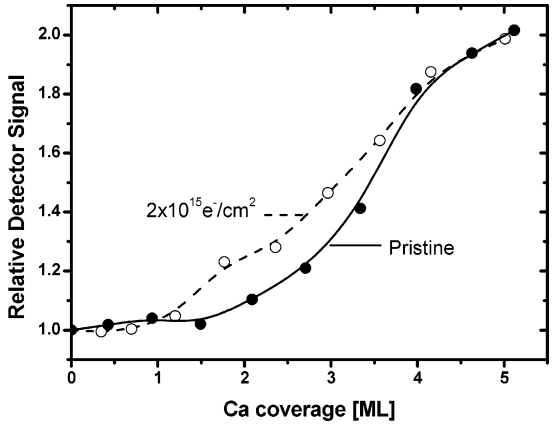

Figure 3. The change in the relative detector signal for pulses of He−Ne laser light of constant intensity (0.07 μJ/pulse) incident on pristine and electron-irradiated PMMA surfaces as a function of Ca coverage at 300 K. The change in signal is due to a change in the absorbance of the laser light incident on the surface. The detector sensitivity is 450 $V/J_{absorbed}$. All measured calorimetric signals were corrected for this increasing contribution to the measured heat signal due to radiation emitted from the hot metal source as the coverage of Ca increases.

after 10 ML of Ca deposition, the Ca ISS intensity has not saturated, indicating that above-surface Ca grows as 3D islands on the PMMA surface that are thicker than 10 ML, separated by Ca-free PMMA.

3.1.3. Sample Optical Absorbency. A correction we need to make to our measured calorimetric heats is to subtract the heat signal from the thermal radiation from the hot effusive metal atom source. Given the constant temperature in the metal oven, its radiation contribution should be constant if the sample optical absorbency does not change with the amount of the adsorbed metal atoms. However, in many cases, adsorbate-induced sample optical absorbency changes have been observed.[30,47,48]

To measure the change in optical absorbency of the sample as Ca is deposited onto the PMMA surface, the response of the heat detector (under the PMMA thin film) to light pulses of constant energy was measured as a function of Ca coverage. Shown in Figure 3 is the sample response to 100 ms pulses of radiation from a He−Ne laser (directed down the same path as the Ca atomic beam) with constant power as a function of Ca coverage on the PMMA. All of the values have been normalized to the initial one. In this case, the relative change in the response directly reflects the relative change of the absorbency.[49] As can be seen, the sample absorbency increases very slowly between 0 and 2 ML of Ca coverage. After 2 ML of Ca adsorbed, the sample optical absorbency increases much faster. The trend in the change of sample optical absorbency as a function of Ca coverage is very similar to that of the Ca ISS intensity, as described above. Together, these two experiments suggest that below 1.5 ML Ca, the majority of the Ca atoms diffuse into the PMMA, but above 2 ML of Ca, large 3D Ca islands mainly grow, above the surface.

Using the measured relative change in the sample absorbency as a function of Ca coverage and the absorbency of a Ca-free PMMA surface (0.13), the normalized absorbency change as a function of coverage was calculated. Taking this into account,

(40) Smithson, R. L. W.; McClure, D. J.; Evans, D. F. *Thin Solid Films* **1997**, *307*, 110.
(41) Zaporojtchenko, V.; Zekonyte, J.; Biswas, A.; Faupel, F. *Surf. Sci.* **2003**, *532*, 300.
(42) Ernst, K. H.; Ludviksson, A.; Zhang, R.; Yoshihara, J.; Campbell, C. T. *Phys. Rev. B* **1993**, *47*, 13782.
(43) Campbell, C. T. *Surf. Sci. Rep.* **1997**, *27*, 1.
(44) Hook, T. J.; Schmitt, R. L.; Gardella, J. A.; Salvati, L.; Chin, R. L. *Anal. Chem.* **1986**, *58*, 1285.
(45) Gardella, J. A. *Appl. Surf. Sci.* **1988**, *31*, 72.
(46) Gregonis, D. E.; Andrade, J. D. In *Surface and Interfacial Aspects of Biomedical Polymers, Surface Chemistry and Physics*; Andrade, J. D., Ed.; Plenum: New York, 1985.
(47) Dvorak, J.; Dai, H. L. *J. Chem. Phys.* **2000**, *112*, 923.
(48) Persson, B. N. *Phys. Rev. B* **1991**, *44*, 3277.
(49) Mandelis, A.; Zver, M. M. *J. Appl. Phys.* **1985**, *57*, 4421.

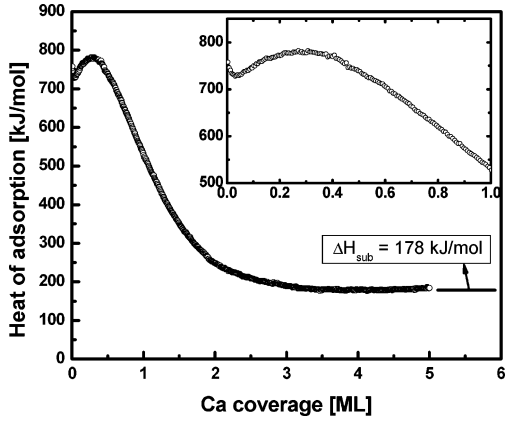

Figure 4. The measured heat of adsorption (standard molar enthalpy of adsorption at 300 K) for Ca adsorption on pristine PMMA at 300 K as a function of Ca coverage. Each data point is due to a pulse of approximately 0.004 ML of adsorbed Ca, with 1 ML defined as the Ca(111) packing density (7.4×10^{14} atoms/cm^2). This is an average of six experimental runs. The inset shows an enlargement of the low-coverage regime.

the amount of radiation absorbed by the sample during Ca deposition was calculated and subtracted from the measured heats.

3.1.4. Heats of Adsorption. The measured standard molar enthalpy of adsorption for Ca onto the pristine PMMA surface at 300 K is shown in Figure 4 as a function of Ca coverage. This is the differential heat of adsorption of 300 K Ca gas. The inset shows the region below 1 ML in more detail. These data are an average of six experimental trials with a standard deviation of 5% in the initial heat value that is attributed to the sample-to-sample inherent differences in our sample preparation technique. The pulse-to-pulse standard deviation in each run (at high coverage, where the heat reaches a constant value) is 1.2 kJ/mol. After averaging runs, this deviation drops to 0.5 kJ/mol. As seen in Figure 4, the heat of adsorption starts at 760 kJ/mol and drops to a minimum of 730 kJ/mol at 0.04 ML. Next, it increases gradually to 780 kJ/mol at 0.3 ML, where it starts to decrease again, and quickly evolves into an exponential-like decay to a final value very close to the bulk heat of Ca sublimation ($\Delta H_{sub} = 178$ kJ/mol[50]) by 3 ML.

The sharp but small and reproducible decrease in the heat of adsorption in the first 0.04 ML is most probably due to a small fraction of surface or near-subsurface defect (or impurity) sites, whose nature we cannot further specify. These more strongly binding sites saturate already by 0.04 ML, which implies they are at very low concentration (<0.04 ML).

Averaging the heat of adsorption for the first monolayer gives a heat of 705 kJ/mol. This is much higher than the heat of sublimation of bulk Ca (178 kJ/mol[50]), indicating that the Ca atoms bond very strongly to the PMMA surface (or near subsurface). As mentioned above, the ester group in PMMA is generally considered as the key chemically active site for metal adsorption.[11−13] Thus, this generally high heat of adsorption up to 1.2 ML is mainly attributed to the binding of Ca atoms to subsurface ester groups. At high coverages (>3 ML), the heat equals the heat of sublimation of Ca, which we attribute to Ca adding to large, 3D Ca islands. This two-state model for adsorbed Ca is consistent with the ISS and absorbency data above.

While each of the six PMMA samples used for Figure 4 showed the same qualitative features versus coverage as Figure 4 (i.e., the small initial drop to a minimum near 0.04 ML, the rise to a maximum of 780 kJ/mol near 0.3 ML, and the final exponential-like decay to Ca's heat of sublimation by 3.5 ML), there was substantial variability in their heats versus coverage curves. Specifically, these features showed the following average values and relative standard deviations (σ): the depth of the low-coverage minimum (730 kJ/mol, $\sigma = 7\%$); the coverage where this minimum occurred (0.04 ML, $\sigma = 43\%$); the coverage at the maximum of 780 kJ/mol (0.3 ML, $\sigma = 27\%$); and the coverage at which the heat had dropped to 450 kJ/mol (1.2 ML, $\sigma = 18\%$). We attribute this to a variation in the defect or impurity concentrations on these PMMA surfaces. In the latter two values, this is mainly an indirect effect, via their influence on the number density of 3D Ca clusters (see below). Interestingly, the heat at the maximum (780 kJ/mol) was very constant ($\sigma = 1.3\%$).

3.2. Ca on Electron-Irradiated PMMA. It is well-known that on polymer surfaces electron or ion beam damage increases the reactivity of the polymer surfaces toward the metals and improves their adhesion.[7,18,32,41,51−54] Ion and electron beam damage have been shown to create bond scission in the PMMA polymer chains, polymer cross-linking, dehydrogenation, deoxygenation, and creation of surface radicals.[18,55−57] In this section, we report studies of Ca adsorption on the electron-irradiated PMMA surface. The procedure for electron irradiation was the same as described previously.[32] The aluminum coating on the PVDF detector, which supports the pristine PMMA film, was held at a positive sample bias of 155 V relative to the hot filament electron source. The PMMA sample was exposed to a measured electron flux of 6 μA/cm^2 for a given time using 155 eV electrons, producing a certain electron dose. This electron flux was constant across the PMMA area studied, and the sample was not annealed after electron irradiation.

3.2.1. Sticking Probability. The sticking probability for Ca on PMMA at 300 K with two different extents of electron damage (2×10^{15} and 1.5×10^{16} e$^-$/cm^2, respectively) is shown in Figure 5 as a function of Ca coverage. Each data set is an average of two experimental runs. Electron irradiation causes an increase in the initial sticking probability, with more electrons increasing the initial sticking probability more. A similar observation was made for Pb adsorption on the electron-irradiated PMMA surface.[32] Both irradiated surfaces show a linear decrease in sticking probability with coverage, followed by an increase to asymptotically approach nearly unity at high coverages. This can be interpreted as a linear combination of three different sticking probabilities for three different types of surface regions present in different amounts at different coverages, as discussed below. These different types of regions will be attributed to: (1) the initial PMMA surface (with or without electron damage), (2) the PMMA surface with a complete layer

(50) Lide, D. R. *CRC Handbook of Chemistry and Physics*, 87th ed.; CRC Press: Boca Raton, FL, 2006.

(51) Zekonyte, J.; Erichsen, J.; Zaporojtchenko, V.; Faupel, F. *Surf. Sci.* **2003**, *532−535*, 1040.
(52) Lhoest, J.-B.; Dewez, J.-L.; Bertrand, P. *Nucl. Instr. Methods Phys. Res., B* **1995**, *105*, 322.
(53) Nowak, S.; Groning, P.; Kuttel, O. M.; Collaud, M.; Dietler, G. *J. Vac. Sci. Technol., A* **1992**, *10*, 3419.
(54) Collaud, M.; Nowak, S.; Kuttel, O. M.; Groning, P.; Schlapbach, L. *Appl. Surf. Sci.* **1993**, *72*, 19.
(55) Bermudez, V. M. *J. Vac. Sci. Technol., B* **1999**, *17*, 2512.
(56) Piganataro, S. *Surf. Interface Anal.* **1992**, *19*, 275.
(57) Adesida, I.; Anderson, C.; Wolf, E. D. *J. Vac. Sci. Technol., B* **1983**, *1*, 1182.

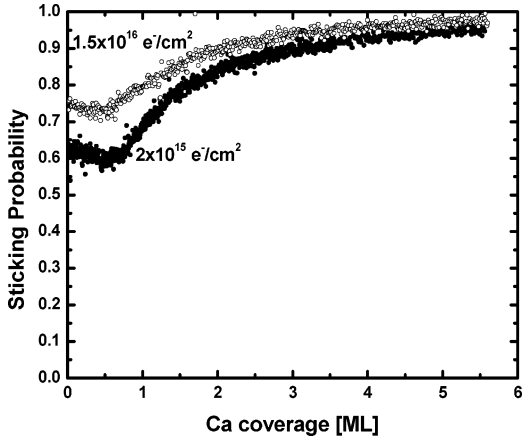

Figure 5. Sticking probability of Ca onto electron-irradiated PMMA surfaces as a function of Ca coverage at 300 K. Each data point represents a pulse of approximately 0.006 ML of Ca coverage at $^1/_2$ Hz. Each data set is the average of two nearly identical data sets from two separate experiments. (Their average relative deviation was 2.2%, which was mostly due to the pulse-to-pulse noise in each run, although in the first 0.6 ML, the values in one run were systematically lower than the other by 5%.)

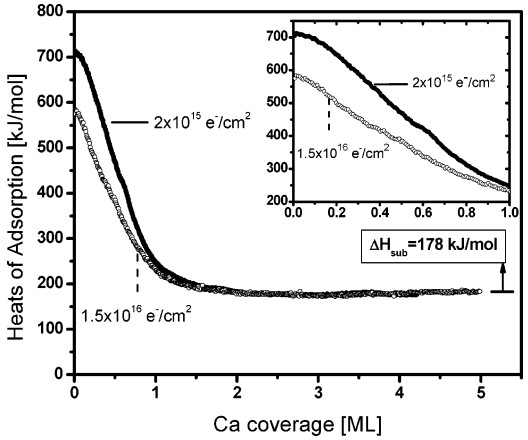

Figure 6. The measured heat of adsorption (standard molar enthalpy of adsorption at 300 K) for Ca adsorption on electron-irradiated, spin-coated PMMA surfaces at 300 K as a function of Ca coverage. Each data point is due to a pulse of approximately 0.005 ML of adsorbed Ca. Each curve is an average of three experimental runs. The inset shows the low-coverage region, 0−1 ML, in more detail.

of subsurface Ca (or more), and (3) solid Ca. The latter two site types are created quasi-sequentially as Ca coverage increases even on pristine PMMA, as noted above. The sticking probability on the initial PMMA surface depends on the e^- fluence, and increases from 0.48 for pristine PMMA to 0.75 for the highest e^- fluence. This suggests that electrons create defects on or near the surface that trap Ca atoms more effectively. Because the ejection of neutrals is much more likely than ions in electron-stimulated desorption, the main defects created on the surface are probably radicals at C centers formed by ejection of H or CH_3 groups.

3.2.2. ISS Experiments and Optical Absorbency. Figure 2 shows the evolution of the Ca ISS peak intensity as a function of Ca coverage for electron-irradiated PMMA surfaces, with these same two electron fluences. As compared to the pristine PMMA surface (● in Figure 2) at the same coverage, the Ca ISS peak intensity is much higher on both electron-irradiated PMMA surfaces, indicating more Ca atoms locate on top of the surface of electron-irradiated PMMA. Moreover, more Ca atoms can be seen in ISS for the higher electron-irradiated PMMA. On both electron-modified PMMA surfaces, the continuous growth in ISS intensity with coverage suggests that the above-surface Ca atoms grow as large 3D islands of low number density on both surfaces, with Ca-free regions between the islands.

We also measured the relative change of the electron-irradiated sample optical absorbency as a function of Ca coverage, using the same method as mentioned above, as shown in Figure 3. Note that the absorbency increases more rapidly with coverage on the electron-damaged surface, consistent with the growth of 3D Ca particles at lower Ca coverage, as also shown by ISS.

3.2.3. Heats of Adsorption. Figure 6 shows the heats of adsorption of Ca atoms onto the electron-irradiated PMMA surfaces as a function of Ca coverage at 300 K. Each curve is an average of three experimental runs. The electron exposures are the same as in Figure 5. As compared to pristine PMMA, the standard deviation in the initial heat values is much smaller, less than 3% for each set. The calorimetric measurements are more reproducible on the electron-irradiated PMMA surface, which suggests that the relative number of defect sites is more constant when created by electron damage than when created by the standard sample preparation of pristine PMMA. This also suggests that the number of defects on pristine PMMA ($<$0.04 ML) are much fewer. In contrast to the defects on pristine PMMA, which appear to have a higher adsorption energy as shown in Figure 4, electron damage creates defects, which appear to have a lower initial heat than on either the pristine surface or its defects. Moreover, the higher is the amount of electron dose, the lower is the initial heat (710 kJ/mol for 2×10^{15} electrons/cm^2 and 580 kJ/mol for 1.5×10^{16} electrons/cm^2). This is not necessarily because these electron-induced defects themselves bind Ca more weakly, but because they lead to more Ca binding simultaneously to 3D Ca clusters, as we explain below. With increasing Ca coverage, the heat decays nearly linearly, with a slope that would drop it to the value of bulk Ca's heat of sublimation (178 kJ/mol) by 1.0 ML. Above 0.8 ML, its decrease slows considerably, so that it asymptotically approaches that value.

4. Discussion

4.1. Ca on Pristine PMMA. This is the first study of any kind addressing the interaction of Ca atoms with PMMA. When a metal is deposited onto a polymer surface, there are several competing processes including trapping, adsorption/reaction, surface diffusion, nucleation of metal clusters, and desorption.[5,7,32]

There are two dominant observations that must be rationalized with any model of Ca growth for coverages below 1.0 ML:

(1) The heat of adsorption is very large (600−800 kJ/mol) in this whole range.

(2) The Ca signal in ISS is only a few percent of the maximum Ca ISS signal observed in this study (see Figure 2), which itself is clearly still smaller than the signal for pure bulk Ca. This implies that less than a few percent of the atoms in the topmost atomic layer are Ca even at 1.0 ML Ca coverage.

We propose the simplest model that is consistent with these facts, whereby the main adsorption mode up to 1.0 ML is for Ca atoms to bond to ester groups just below the PMMA surface,

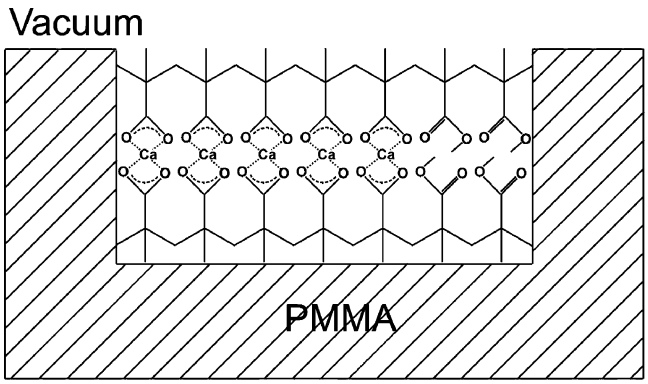

Figure 7. A schematic drawing of Ca bonded to subsurface ester groups of PMMA in the proposed model for the state that has a heat of Ca adsorption of 780 kJ/mol but contributes negligibly to the Ca ISS signal. We show a Ca:ester stoichiometry of 1:2, whereby each Ca instead reacts with two ester groups to make the carboxylate, $(R-COO)_2Ca$, and release ethane gas, as proposed in the Discussion based on the measured reaction energy. We show here only a low-coverage, but this state eventually populates 4−6 ester layers at high coverage, where 3D Ca(solid) particles also grow on top of the surface.

which mainly exposes methyl and methylene groups.[18,44−46,58] We assume that this Ca is just below the surface (as opposed to far below the surface) because Ca was seen at low coverage with more intensity in its AES peak than in its ISS peak, both relative to high coverage. (The escape depth of the 292 eV electrons in this AES peak is 1 nm.)

It is useful to estimate how many of these ester groups are present per unit area on the starting PMMA surface. The bulk density of PMMA (1.2 g/cm^3) implies a packing density of 7.2 $\times$ 10^{21} monomers units per cm^3. If we further assume that the surface of PMMA is a closest-packed plane of these monomer units, like the (111) face of a FCC crystal, the density of the surface monomer units is 3.4 $\times$ 10^{14} monomers/cm^2. At this density, if one Ca atom bonded to every ester group in this topmost layer of monomer units, it would give a Ca coverage of 0.46 ML, remembering our definition of one ML (7.4 $\times$ 10^{14} atoms/cm^2). If each Ca atom instead binds to two ester groups to make the Ca carboxylate, as we suggest below, a Ca coverage of 0.23 ML would correspond to completion of the reaction with every ester group in this topmost layer. It is very interesting that this coverage is very close to that where the maximum heat of adsorption is observed in Figure 4 (780 kJ/mol at 0.3 ML). Although the heat decreases after this maximum, it still remains much higher than the bulk sublimation energy of Ca up to 2 ML, implying that much more than one layer of subsurface ester groups eventually react. A schematic drawing of the subsurface Ca−ester complexes is shown in the Figure 7. In this model, each Ca reacts with two ester groups, as justified below. Diffusion of Ca into polymer films at room temperature has been reported for Ca on PPV.[59,60]

At Ca coverages from 3 to 8 ML, there are two key observations:

(1) The heat equals the sublimation energy of bulk Ca.

(2) The ISS signal for Ca increases nearly linearly with Ca coverage, but a large fraction of the surface (90% → 60%) still remains Ca free. This can be seen in Figure 2, where the Ca ISS signal is only 10% → 40% of the value expected for a pure Ca film (i.e., its saturation value.)

This shows that the Ca here is mainly adding to large 3D Ca particles of low number density on the PMMA surface. If the Ca signal per unit Ca particle/PMMA interface area is independent of particle size, its linear increase would imply that the Ca particle density is also increasing slowly.

The decrease in heat beyond the maximum at 0.3 ML up to 3 ML in Figure 4 is most simply explained as the simultaneous population of both of these two main types of Ca sites: subsurface ester groups (now below the first ester layer) and sites on 3D Ca particles above the PMMA surface. The observed heat at any coverage above the maximum reflects the fraction of Ca that goes to each of these two types of sites, with the probability that it populates subsurface esters decreasing toward zero as their Ca-occupied depth increases beyond two layers. Note that the kinetic competition between the population of these two types of sites occurs on the time scale of the heat pulse transients or faster (<0.10 s), implying that Ca atoms initially trap in a weakly held precursor state where it rapidly diffuses across the surface, and even into the subsurface (and possibly back out). As it diffuses, it can add to a growing Ca particle, or react with a subsurface ester group, or desorb. Assuming that 100% of the Ca atoms that hit the surface get trapped in this precursor state, the sticking probability of 0.8 in this coverage range implies that about 20% of the precursors desorb. As the Ca coverage increases, the fraction of the surface covered by Ca particles increases, so that this fraction that desorbs decreases eventually to near zero, and the fraction that add to 3D Ca particles increases to eventually reach 100%. Note also that the time scale for desorption is extremely fast (<5 ms, see above), implying that the whole kinetic competition between the three available pathways (desorbing, attaching to a subsurface ester, or adding to a growing 3D cluster) is complete in <5 ms.

When the first pulse of Ca impinges on the pristine PMMA surface, three processes occur in competition: diffusion to intrinsic defect sites (which may be subsurface), diffusion into the subsurface to find normal ester groups, and desorption from the surface. The defect sites are quickly saturated (<0.04 ML).

The increase in heat of adsorption with Ca coverage from 0.04 to 0.3 ML in Figure 4 can be explained by attractive interactions between subsurface Ca−ester complexes. That is, these complexes are more stable as islands than as isolated entities. Because Ca bonding to the ester group is probably at least partially ionic, the interactions between such complexes probably result in bulk-salt-like ionic attractions, as shown schematically in Figure 7. Therefore, in Figure 4 the heat of adsorption increases as the population of subsurface Ca sites increases, until it reaches a maximum of 780 kJ/mol. Extrapolating the linear part of this increase (between 0.07 and 0.15 ML) back to zero coverage gives a heat of 710 kJ/mol, which provides an estimate of the heat of binding of Ca in an isolated subsurface Ca−ester complex. The maximum net attraction between subsurface Ca−ester complexes occurs at 0.3 ML and is 780−710 = 70 kJ/mol. The initial heats that lie above this extrapolated line can be explained by Ca binding at 0.02 ML of defect sites with a fixed heat of adsorption of 760 kJ/mol.

After the top layer of subsurface ester sites gets filled, there is a kinetic competition between continuous Ca bonding to

(58) Wang, J.; Chen, C.; Buck, S. M.; Chen, Z. *J. Phys. Chem. B* **2001**, *105*, 12118.
(59) Janssen, F. J. J.; van Ijzendoorn, L. J.; van der Gon, A. W. D.; de Voigt, M. J. A.; Brongersma, H. H. *Phys. Rev. B* **2004**, *70*, art. no. 165425.
(60) Janssen, F. J. J.; Denier van der Gon, A. W.; van IJzendoorn, L. J.; Thoelen, R.; de Voigt, M. J. A.; Brongersma, H. H. *Appl. Surf. Sci.* **2005**, *241*, 335.

deeper ester groups versus Ca addition to 3D Ca particles. Because diffusion into a deeper PMMA layer takes longer and because the fraction of the surface covered by 3D Ca clusters increases with Ca coverage, the kinetic competition to add to 3D clusters gets more and more probable as coverage increases, even though the bonding between Ca and subsurface ester groups is much stronger. It is also possible that Ca interacting with the surface causes a change in the surface structure or defects, which could make it easier to grow 3D Ca particles on the surface. Once bonded to a 3D Ca cluster, the Ca is kinetically prevented from moving off the Ca particle to subsurface ester sites, at least on the time scale of these experiments.

Neglecting the high heat of adsorption generated by saturating the small amount of surface intrinsic defect sites with Ca, we can reproduce the major features of the data with a simple model that assumes that the measured heat of adsorption as a function of Ca coverage is composed of only two different heats of adsorption generated by two types of adsorption: (1) Ca bonded to subsurface ester groups that have the highest observed heat of adsorption (780 kJ/mol, where each Ca−ester complex is experiencing its maximum attraction to its neighbor complexes), and (2) Ca in large 3D Ca(solid) particles on the surface that have the bulk heat of sublimation (178 kJ/mol). Using a linear combination of these two sites, we can semiquantitatively reproduce the coverage dependences of both the heat data in Figure 4 and the ISS data in Figure 2. According to this model, the measured heat of adsorption can be expressed as the following:

$$\Delta H_{ads} = f_A \cdot \Delta H_{ads,A} + (1 - f_A) \cdot \Delta H_{ads,B} \qquad (1)$$

where A represents subsurface ester groups, B represents sites on large 3D Ca islands, f_A is the fraction of the adsorbed Ca atoms in each pulse that bonds to A sites, $\Delta H_{ads,A}$ is the heat for Ca at A sites (780 kJ/mol), and $\Delta H_{ads,B}$ is the heat for Ca on B sites (178 kJ/mol). The heat data in Figure 4 for Ca coverages above the maximum at 0.3 ML were fitted to Eq 1 to determine f_A at each pulse. Below 0.3 ML, we assumed that f_A is 1.0, because the Ca ISS signal is still negligible in that coverage range. Once f_A is known from this fit to Eq 1, the Ca coverages in these two site types can be calculated versus total Ca coverage by multiplying f_A or $(1 - f_A)$ by the sticking probability and the Ca flux, and summing all of the pulses up to the coverage of interest. Figure 8 shows the coverages of A and B sites calculated in this way. Also shown are the results from the electron-irradiated PMMA surface, which will be discussed later.

As can be seen, all of the adsorbed Ca atoms diffuse subsurface to bond with the ester groups below 0.5 ML. Above 1 ML, the population of these sites starts to saturate, and by 2.5 ML it fully saturates with a total coverage of 1.23 ML of subsurface Ca. This is equivalent to bonding one Ca atom to each ester group in 2.6 layers of monomers in PMMA (assuming closest-packed monomer spheres as described above). If each Ca reacts with two ester groups, which is highly probable as explained below, then this is equivalent to reacting with 5 layers of monomers in PMMA. As these sites approach their maximum population (probably due to diffusion limitations on their rate of occupation), the Ca coverage starts to grow in 3D clusters, which are the only growing species above 2.5 ML total Ca.

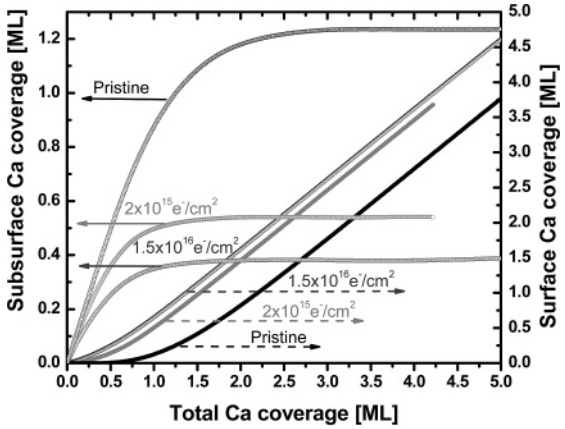

Figure 8. Evolution of the coverages of Ca in the two types of sites (i.e., bonded to subsurface ester groups or to above-surface 3D Ca clusters) as a function of total Ca coverage on pristine and electron-irradiated PMMA surfaces at 300 K. These site coverages were derived from the coverage-dependent heats of adsorption, assuming that only these two sites are populated and they each have a constant heat of adsorption (780 and 178 kJ/mol, respectively). See text for details.

Using these A and B site coverages in Figure 8, we now can predict the Ca ISS intensity as a function of Ca coverage. We assume that subsurface Ca (A site) does not contribute to the Ca ISS signal and that each Ca atom in 3D Ca clusters contributes the same signal to ISS. This latter assumption is equivalent to assuming that the 3D Ca clusters are the same size, independent of coverage, or at least have the same average ratio of volume to area (projected onto the PMMA surface plane). The solid line in Figure 2 shows the calculated result. This agrees very well with the experimental data, strongly supporting this simple two-site model. Note that the *y*-axis was multiplied by a scaling factor to get this agreement in Figure 2. The scaling factor was 6.2% per ML. This factor implies that each Ca atom in the 3D clusters contributes <6.2% of the Ca ISS signal it would contribute if it were instead in a single, closest-packed layer of Ca atoms. This in turn implies that the 3D Ca islands are, on average, >1/0.062 = 16 atomic layers thick. Furthermore, the optical absorbency/reflectivity changes as a function of Ca coverage are qualitatively consistent with this model.

The heat of 780 kJ/mol for binding to subsurface ester groups is much higher than the bond energy of most of the chemical bonds in PMMA,[61] suggesting that polymer bonds may be breaking upon Ca deposition. For comparison, the standard heats of formation of some solid compounds of Ca, from Ca(solid), are: 181.5 kJ/mol for CaH_2,[50] 634.9 kJ/mol for CaO,[50] 1207.8 kJ/mol for $CaCO_3$,[50] 985.2 kJ/mol for $Ca(OH)_2$,[50] and 1360 kJ/mol for CaC_2O_4.[50] To account for the energy difference between Ca(solid) and Ca(gas), all of these energies should be lowered by 178 kJ/mol to compare to our heats. Among the many possible reactions we considered that could occur upon Ca adsorption, our measured heat agrees best with its reaction to form the calcium carboxylate and release ethane gas:

$$Ca(g) + 2R{-}COOCH_3(s) \rightarrow (R{-}COO)_2Ca(s) + CH_3{-}CH_3(g)$$

where R represents the main polymer chain. Using the simpler example where R− equals CH_3−, we estimate the standard

(61) Huheey, J. E. *Inorganic Chemistry*, 3rd ed.; Harper & Row: New York, 1983.

enthalpy of this reaction to be −855 kJ/mol, which is very close to the observed enthalpy of −780 kJ/mol. This is calculated from the following standard heats of formation: $Ca(g) = 178$,[50] $CH_3COOCH_3(l) = -446$,[50] $(CH_3COO)_2Ca(s) = -1485$,[62] and $CH_3CH_3(g) = -84$,[50] all in kJ/mol and at 298 K. One could confirm this mechanism by monitoring the amount of ethane gas released during Ca adsorption. This suggests that future experimentalists who study metal adsorption on polymers should routinely look for such gas-phase products, which to our knowledge has never been done.

4.2. Ca on Electron-Irradiated PMMA. This same simple two-site model can be used to semiquantitatively reproduce the heat and ISS date for the electron-damaged surfaces as well. Again, the heat data (Figure 6 here) were fitted to Eq 1 to obtain the fraction of adsorbed gas that goes into each type of site with each pulse (now starting already from zero coverage). This was multiplied by the Ca flux and the sticking probability and integrated with time, to give the separate coverages of Ca in A and B sites versus total Ca coverage shown in Figure 8. As with pristine PMMA, mainly subsurface (A) sites are populated at the lowest coverage. However, the growth of Ca in 3D particles is seen at much lower coverage for the electron-damaged PMMA, and is already populated with some probability from the lowest coverage. We attribute this to electron-induced defects on the PMMA surface, which act as nucleation sites to facilitate growth of more 3D Ca particles. This also explains the increase in the initial sticking probability with electron damage.

A very important result in Figure 8 is the fact that the subsurface Ca−ester complexes saturate on the electron-damaged surfaces at coverage of only 0.40−0.53 ML. This is very similar to the coverage of 0.46 ML that corresponds to one Ca atom bonded to every ester group in this topmost layer of monomer units (or in the two topmost layers, if the binding stoichiometry is 2:1 as suggested above if the carboxylate is formed). This implies that, for these electron-damaged surfaces, only the topmost layer (or two) of monomer units gets populated. We attribute this to the greater density of 3D Ca clusters as compared to pristine PMMA, which trap diffusing Ca atoms faster and kinetically prevent them from diffusing to deeper layers to find ester groups there.

We used these A and B site coverages in Figure 8 to predict the Ca ISS intensity as a function of Ca coverage for the more heavily damaged surface, just as we did above for pristine PMMA. The dashed line in Figure 2 shows the calculated result, which again agrees excellently with the ISS data and strongly supports this simple two-site model. Again, the *y*-axis was multiplied by a scaling factor to get this agreement in Figure 2, but the scaling factor was 9.7% per ML here, as compared to 6.2% per ML for pristine PMMA. This factor implies that the 3D Ca islands are, on average, >10 atomic layers thick, as compared to >16 layers on pristine PMMA. Thus, the Ca particles on the electron-damaged surface are thinner (and therefore probably also smaller in diameter) than the clusters on pristine PMMA. This is consistent with our proposal above that electron damage creates defect sites that act as nucleation centers for these 3D Ca clusters. This will result in more, smaller Ca clusters at the same Ca coverage.

Similar enhanced nucleation was found for Cu adsorption on ion-damaged PMMA surfaces.[18] Electron irradiation to the PMMA surface causes the formation of various surface defects,[18,55−57] for example, surface radicals. Moreover, the more electrons that are exposed to the PMMA surface, the more defects are created. These defects sites can act as the nuclei for metal condensation, as observed for Pb on electron-irradiated PMMA.[32]

In contrast to the pristine PMMA surface, the sticking probability of Ca (*S*) on both electron-irradiated PMMA surfaces starts high, linearly decreases to 0.6 or 0.73 at coverage of 0.5 ML, and then increases slowly toward unity. In the initial region up to 0.5 ML, most of the adsorbing Ca is populating subsurface ester sites, although a significant number populate 3D Ca clusters. The linear decrease in *S* here as the first layer of subsurface sites gets filled indicates that the intrinsic sticking probability is lower onto a surface that has the first subsurface layer of ester groups completely occupied with Ca than when these sites are still empty on the e^--damaged PMMA surface. The opposite is true for pristine PMMA. The sticking probability at the coverage where one layer of subsurface ester groups is occupied (0.5 ML) is very similar on all three surfaces, varying only between 0.6 and 0.73. This seems to be a value characteristic of such a surface, nearly independent of electron damage. The sticking probability varies much more between these three surfaces when no Ca is yet present (i.e., S_0), increasing from 0.48 to 0.75 with electron dose. As noted above, this is partially due to the creation of defect sites by electrons that nucleate more 3D Ca clusters on the surface, although their number density is still very low. Initially, about 75% the adsorbing Ca is going to subsurface esters on this e^--damaged surface, and only 25% are going to 3D Ca clusters, according to Figure 8. The fraction that is going to 3D Ca clusters seems too low to explain the 56% increase in S_0. This implies that the rate constant for those that go to subsurface ester sites must also be increased by the electron dose. Perhaps this is due to damage to the ester groups themselves or creation of more facile diffusion pathways for migrating Ca atoms to find subsurface ester groups.

By a total coverage of 0.5 ML, about one-half of the Ca resides in thick 3D clusters and one-half in subsurface ester sites on the most heavily damaged PMMA surface, according to Figure 8. The observed decrease in *S* as the total coverage increases to this condition must reflect a complex combination of: (1) a decrease in *S* for those that go to subsurface esters, due to the increasing population of first-layer subsurface Ca, (2) an increase in *S* for the fraction that stick to 3D clusters as their size and number density grow, and (3) an increase in *S* due to the increasing fraction that stick to 3D clusters. The linear decrease suggests that the first of these effects dominates, so that the observed decrease is essentially a Langmuir-type site-filling model.

5. Conclusion

Combining adsorption microcalorimetry, sticking probability measurements, and ISS provides a powerful approach for elucidating the growth of metal films on polymer surfaces, as demonstrated here for the case of Ca on PMMA. Gaseous Ca traps in a weakly adsorbed precursor state, which diffuses across and into the PMMA surface to eventually either desorb or bind to one of the two dominant types of sites it populates: (1)

(62) Franzosini, P.; Sanesi, M. *Thermodynamic and Transport Properties of Organic Salts*; Pergamon Press Inc.: New York, 1980.

subsurface ester groups, which with it reacts with very high heat of adsorption (initially 710 kJ/mol), or (2) large 3D Ca clusters, with a lower heat of adsorption, equal to Ca's bulk sublimation enthalpy (178 kJ/mol). The subsurface Ca−ester complexes have mutually attractive interactions, so that their heat of adsorption increases to 780 kJ/mol as their coverage increases in the first subsurface layer. Eventually Ca binds to 4−6 layers of these subsurface ester groups at saturation (assuming each Ca reacts with 2 esters to form the Ca carboxylate), after which Ca only grows on top of the surface, eventually as a solid Ca thin film. The initial sticking probability of Ca on the pristine PMMA surface is surprisingly low ($S_0 = 0.5$), but this increases with electron damage due to creation of defects that (1) nucleate more 3D Ca clusters and (2) increase the rate constant for Ca moving to subsurface ester sites. The same two dominant site types are populated by Ca on electron-damaged PMMA, but the formation of 3D clusters is more favored in their kinetic competition, so that only two layers of subsurface ester groups get populated at saturation.

Acknowledgment. The National Science Foundation is acknowledged for financial support of this study. In addition, we would like to acknowledge Winston Ciridon in the Department of Bioengineering, University of Washington, for his assistance in spin coating the samples.

JA067437C